

Deep Learning for Autism Detection Using Eye Tracking Scanpaths

Supritha R

Department of Computer Science and Engineering
Amrita School of Computing
Amrita Vishwa Vidyapeetham, Chennai, India
Email: ch.en.u4aie20066@ch.students.amrita.edu

Bharathi Mohan G

Department of Computer Science and Engineering
Amrita School of Computing
Amrita Vishwa Vidyapeetham, Chennai, India
Email: g_bharathimohan@ch.amrita.edu

Abstract—Autism spectrum disorder (ASD) is a neurodevelopmental condition marked by difficulties in social interaction, communication, and limited repetitive behaviors, with symptoms varying significantly among individuals. Eye tracking holds promise in autism detection due to its unique ability to capture and analyze visual attention patterns, providing insights into the cognitive processes and atypical visual behaviors associated with ASD. Eye-tracking technology offers a unique perspective, allowing the observation and quantification of visual attention patterns, which may reveal distinctive features associated with ASD. These visualizations represent how individuals, particularly those with ASD, explore and engage with stimuli. In this research, we propose a novel approach using deep learning models, specifically DenseNet-201, EfficientNet B7, ResNet-50, and MobileNetV2, to analyze eye-tracking scan paths for ASD detection. The dataset focuses on visualizations of eye-tracking scan paths, primarily involving individuals with ASD. The study yielded promising results, with the deep learning models achieving accuracies of 94.97%, 94.74%, 84.21%, and 92.45%, respectively. DenseNet-201 demonstrated the highest accuracy at 94.97%. The research contributes to advancing early diagnosis and intervention strategies for individuals with ASD.

Index Terms—Autism spectrum disorder, Typical Control, Deep learning, eye tracking

I. INTRODUCTION

Autism spectrum disorders (ASD) encompass a collection of neurodevelopmental conditions characterized by restricted and repetitive interests and activities, along with persistent challenges in social communication. According to a 2018 investigation conducted by the Centers for Disease Control and Prevention (CDC), 59 out of every 100 American children display signs indicative of ASD. In the Republic of Korea, the projected prevalence of ASD among school-age children stands at 2.64% [1]. Diagnosing autism is challenging due to the absence of distinct physical characteristics in affected children. Typically, physicians employ screening tools designed for early childhood to detect autism in children aged 16 to 30 months. However, the lack of experience and insufficient training among clinicians has resulted in inaccurate ASD diagnoses in some cases. The absence of a straightforward identification method for ASD can deter parents from pursuing screening for their children. Achieving an accurate diagnosis necessitates regular follow-up treatments for each ASD patient. Nonethe-

less, since assessments rely on subjective observations, there remains a risk of physicians incorrectly determining the functional levels of ASD [2]. The increasing prevalence of autism spectrum disorder (ASD) has led to a diverse range of diagnostic approaches, including both traditional screening scales and advanced technological methods. Technology-driven techniques, particularly those involving eye trackers, are transforming conventional subjective methods into objective ones, enabling early ASD screening and intervention. Eye gaze irregularities are identified as reliable ASD biomarkers through eye trackers [3]. The development of the brain is influenced by experience-dependent mechanisms, making a child's focus a crucial factor in shaping brain development. Utilizing eye tracking as a technology to measure a child's visual attention offers potential for uncovering prognostic indicators [4]. Deep learning, a subset of AI, has emerged as a powerful tool for medical image analysis, capable of learning from vast image datasets. In this study, we introduce an innovative approach that employs state-of-the-art deep learning models, including DenseNet-201, EfficientNet B7, ResNet-50, and MobileNetV2, to meticulously analyze eye-tracking scan paths for the purpose of ASD detection. The dataset utilized in this research primarily comprises visualizations of eye-tracking scan paths, specifically emphasizing individuals diagnosed with ASD. The outcomes of the investigation are highly promising, as the deep learning models exhibited notable accuracies of 94.97%, 94.74%, 84.21%, and 92.45%, respectively. Particularly, the novelty of this work lies in utilizing complex model Densenet-201 and Efficientnet B7 and applying fine tuning, showcasing the highest accuracies at 94.97% and 94.74%. This research significantly contributes to the advancement of early diagnosis and intervention strategies tailored for individuals grappling with ASD and also emphasizes the power of various pre-trained deep learning models in analyzing the scanpaths efficiently as showcased in results and promises to open doors for further research in autism detection using eye tracking scan paths. The rest of the paper is structured as follows: related works, proposed methodology, results and discussion, conclusion, future scope and references to discuss the relevant works done previously, data and algorithms used, results obtained, contribution and further research scope of this work.

II. RELATED WORKS

By observing how adults with and without high-functioning autism interact with websites, this study [5] focuses on autism detection. To explore gaze-based and other characteristics, machine learning models were trained on 71 individuals' eye-tracking data from two investigations using logistic regression models. According to the findings, autism may be identified automatically with 74% accuracy. This paper [6] integrates VAM and AI approaches to provide a computational strategy for eye tracking-based ASD diagnosis. Significant gains are made in recall (69%), specificity (93%), and precision (90%) using the supervised classifier. In this work [7], 37 (TD) and 37 ASD children, ages 4-6, are the subjects of an investigation into the possibility of eye tracking for early ASD detection. The 10-second video shows significant reductions in children with ASD in fixation times at six regions of interest. With discriminant analysis, the algorithm successfully classifies data with an impressive 85.1% classification accuracy, 86.5% sensitivity, and 83.8% specificity.

This study [8] employs three AI techniques—DL, ML, and a hybrid ML-DL method—to detect ASD via eye tracking. The first approach, which achieves an amazing 99.8% accuracy, uses feature categorization using LBP and GLCM for FFNNs and ANNs. The second approach uses pre-trained CNN models to achieve high accuracies of 93.6% and 97.6%, respectively. By integrating SVM with CNN, the third technique obtains accuracies of 95.5% and 94.5%. This work [9] examines the usefulness of eye-tracking information gathered during face-to-face interactions for precisely categorizing kids with ASD and TD. Using four ML models (ML)—SVM, decision tree, random forest, and linear discriminant analysis—the SVM classifier stands out with an optimal accuracy. In order to explore the possibility of eye-tracking techniques as an early biomarker for autism, this study [10] applies machine learning algorithms to a dataset comprising 547 eye-tracking scan pathways from children who are usually developing and autistic. The deep neural network model outperforms conventional machine learning techniques.

This study's [11] objective is to use machine learning to detect ASD in children. Ninety-seven kids between the ages of three and six were enrolled in the study, and eye-tracking and EEG data were used as data for an SVM classifier. The EEG data underwent power spectrum analysis, whereas the eye-tracking data underwent face gaze analysis, which involved concentrating on AOI. The combined use of EEG and eye-tracking data yielded a notable classification accuracy when 32 features were selected. The study [12] examines the use of eye-tracking techniques in a VR setting to differentiate children with autism from generally developing children based on their visual attention habits. Unique visual preferences are shown by children with autism, such as a preference for the faces of adults over those of children and a stronger interest in adults than in other children. Multivariate supervised ML models are used in the study. A novel machine learning classifier for autism detection is introduced in the paper [13], which

focuses on eye movement sequences on web pages. By adding sequential data and using Scanpath Trend Analysis (STA) to find trending paths in both neurotypical and autistic individuals, it overcomes the shortcomings of earlier classifiers, non-sequential data approaches and gives stable accuracy.

In an effort to provide a portable and affordable tool, the study [14] investigates the use of the smartphone-based eye-tracking algorithm, iTracker, for tracking gaze behavior in ASD patients. Tests conducted on volunteers in good health show that iTracker is accurate in differentiating between gaze directed at the mouth and eyes. The study [15] suggests using eye-tracking patterns converted into visual representations as part of a machine learning approach for the early diagnosis of ASD in children. The study uses simple neural network models to treat the diagnosis as an image classification task, and it achieves a notably high classification accuracy with an AUC greater than 0.9. In the paper [16], a novel approach to measuring the usefulness of visual information extracted from facial stimuli in emotion recognition is presented, with special attention to how participants with autism differ from typically developing people. Using eye-tracking technology, the autistic group showed less attention on the eyes and more fixations on lower facial regions than the typically developing group. The study shows, there may be a relationship between the inability of autistic people to recognize emotions and their tendency to extract visual information through eye fixations. According to the study [17], eye-tracking data on altered patterns of visual social attention preference can be used to identify sensitive biomarkers for ASD. The most successful eye-tracking protocol was the dancing people versus dynamic geometry paradigm, which was evaluated in young Chinese children with ASD and their typically developing peers. Children with autism showed a decreased visual preference for dancing individuals and a greater preference for geometric patterns. The purpose of the study [18] was to evaluate how children with autism spectrum condition (ASC) could recognize emotions and eye gaze patterns when presented with avatar faces instead of real faces. Based on the type of stimulus and the expressed emotion, children with ASC showed increased emotion recognition accuracy and were more drawn to particular facial regions (mouth or eyes). ASC patients may benefit from avatar faces because they can improve facial recognition, especially when those faces convey negative emotions. With an emphasis on social and non-social images, the study [19] sought to compare the visual attention patterns of young children with ASD and typical controls. Compared to controls, children with ASD showed a marked emotional bias, showing a delayed orientation to angry faces and a preference for happy faces, but they also paid much less attention to faces in general. Using head-mounted eye tracking, the study [20] sought to understand how children with ASD coordinate manual actions and visual attention during toy play. Surprisingly, the study did not find any significant differences in the way that children with ASD and typically developing (TD) children distributed their visual attention, produced manual actions, or coordinated their manual and visual behaviors when playing with a parent.

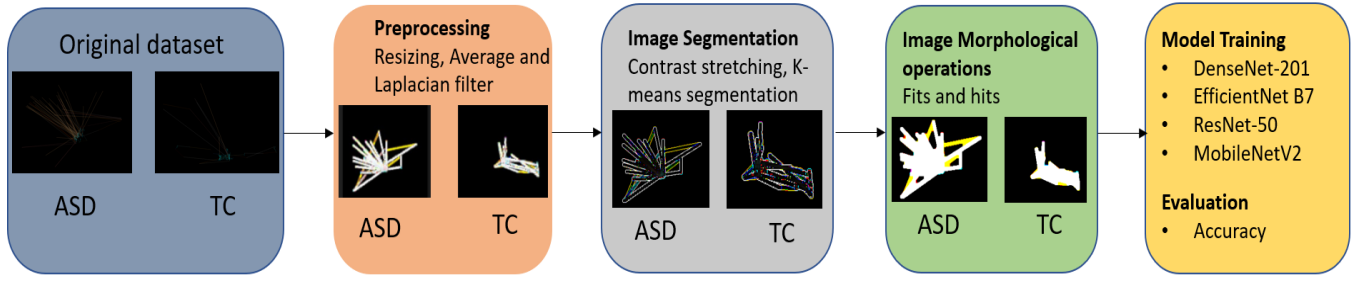


Fig. 1: Block diagram description of the proposed framework.

III. PROPOSED METHODOLOGY

The first part of the research entails thorough preprocessing of the dataset images to improve their analytical suitability. This includes the essential processes of resizing the photos and using Laplacian and average filters to minimize noise and guarantee the best possible data quality. After that, the image is segmented using the k-means segmentation technique, which is a commonly used technique for dividing images into discrete segments and applying contrast stretching to improve the contrast of the image. After segmentation, the processed images are further refined by performing image morphological operations, namely adjacent intersection and adjacent union test. The improved photos are then split into train and test datasets with an 80:20 ratio and shuffled before being fed into deep learning models such as DenseNet-201, EfficientNet B7, ResNet-50, and MobileNetV2 and fine-tuning is also performed. The accuracy of these models is used to assess their performance. Fig 1 illustrates the suggested methodology.

A. Dataset

The visual representations of eye-tracking scan paths, of ASD and TC, comprise the dataset utilized in this study. The basic idea is to use image analysis techniques to convert the subtleties of eye movements into observable visual patterns, which will make diagnostic tasks easier to complete. Scanpath includes tracking of frequent rapid eye movements and pauses in movement. 59 children's scanpath data is taken, also to to facilitate early detection, young school kids' with average age of 8 eye tracking data was included. As of right now, the dataset consists of 547 images, all of which were originally set to 640x480 as their default size. Two discrete classes are discernible in the dataset: i) 'TCImages,' signifying individuals who do not have ASD (Non-ASD or TC), and ii) 'TSImages,' signifying those who have been diagnosed with ASD. The dataset specifically consists of 219 images that correspond to people with an ASD diagnosis and 328 images that correspond to participants without an ASD. Fig 2 displays the input images.

B. Image Preprocessing

In the image preprocessing stage, several techniques are used to enhance the quality and reduce noise in the input

images. First step involves resizing of the images to a standard dimension of 224 by 224. This is followed by applying to key filters: average and Laplacian filters. The average filter is a standard image processing method to smoothen and reduce noise in the images. It is implemented with the help of a convolution operation with a kernel (filter) that determines the mean value of pixels within a specified neighborhood. The formula for average filter is described as follows:

$$I(x, y) = \frac{1}{ab} \sum_{c=1}^a \sum_{d=1}^b J(x-c, y-d) \quad (1)$$

where $I(x,y)$ is the resultant average filtered pixel value given original pixel value $J(x,y)$, and a and b indicate the dimensions of the filter kernel.

The Laplacian filter is used for enhancing edges and intensity of an image. Similar to mean filter, it is implemented with the help a convolution operation with a kernel(Laplacian). Laplacian filter can be expressed as:

$$\nabla^2 A(a, b) = \frac{\partial^2 A}{\partial a^2} + \frac{\partial^2 A}{\partial b^2} \quad (2)$$

To get the final enhanced image, the Laplacian-filtered image is subtracted from the Average-filtered image. The following is the stated procedure:

Optimized Image = Average Filtered Image – Laplacian Filtered

Mathematically, the above equation is written as:

$$Z(i, j) = X(i, j) - Y(i, j) \quad (3)$$

where the pixel values for the average-filtered image are denoted by $X(i,j)$, the pixel values for the Laplacian-filtered image are represented by $Y(i,j)$, and the optimized image is denoted by $Z(i,j)$. Fig 3 presents the results of preprocessing.

C. Image Segmentation

Image segmentation is used to ease the process of interpreting the visual content contained in an image. In order to improve the contrast in the image and facilitate K-Means' ability to recognize and cluster similar pixels, contrast stretching is first applied. One method that is frequently used for segmenting images is K-Means clustering. The objective is to

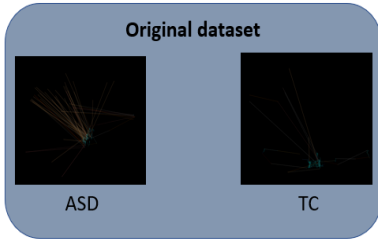


Fig. 2: Original dataset

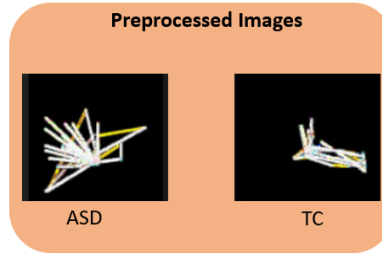


Fig. 3: Preprocessed Images

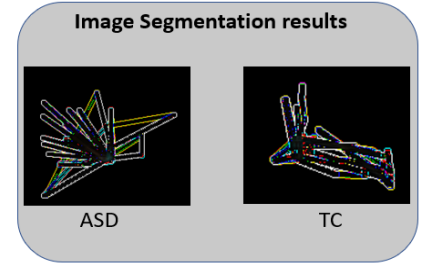


Fig. 4: Image Segmentation Results

divide the pixels of an input image I into K clusters according to similarity. The sum of squared distances between each pixel and its designated cluster center is minimized by the K-Means algorithm. Here is a method to formulate the algorithm:

$$\text{Min } T = \sum_{a=1}^A \sum_{b=1}^B ||Z^a - \mu_b||^2 \quad (4)$$

where:

A = number of pixels in the image,

Z^a = vector representing the i -th pixel,

μ_b = vector representing the j -th cluster center.

The method creates a segmented image by matching each pixel to the nearest cluster center for each clustering iteration. Proper segmentation is essential to precise image analysis. The negative sum of squared distances, which measures how compact the clusters are, is a frequently used metric. Calculating the segmentation score S is as follows:

$$S = (-T) \quad (5)$$

The degree to which the K-Means algorithm has successfully clustered the pixels is indicated by the negative sum of squared distances (S). More compact clusters are indicated by a lower value, which suggests better segmentation.

Finding the segmentation that minimizes J and, as a result, maximizes S is the goal. The segmentation with the highest score is determined by the algorithm iterating over a range of cluster values (K). The segmentation with the maximum S is the best segmentation I_{best} :

$$I_{best} = \arg \max_S \{S(K)\} \quad (6)$$

where the segmentation score for a given K is denoted by $S(K)$. Fig 4 displays the outcomes of the image segmentation process.

D. Image Morphological Operations

In the image processing pipeline, image morphological operations are employed to refine the segmented regions obtained through previous processes. Specifically, adjacent union tests, referred to as "fits," and adjacent intersection tests, referred to as "hits," are sequentially applied with a kernel size of 5×5 . Morphological operations play a crucial role in shaping, enhancing, and extracting meaningful structures within the segmented regions. The fits operation involves the dilation of

adjacent regions, where the dilation operation (δ) is defined as:

$$(f\delta g)(x, y) = \bigvee_{(s, t) \in E_g} f(x - s, y - t) \quad (7)$$

The operation $(f\delta g)(x, y)$ represents the segmented image, where g is the structuring element (kernel) with pixel coordinates (x, y) . The union (\bigvee) operation is applied over the (s, t) in set E_g defined by the structuring element. Subsequently, this operation achieves the erosion of adjacent regions:

$$(f\epsilon g)(x, y) = \bigwedge_{(s, t) \in E_g} f(x + s, y + t) \quad (8)$$

The operation $(f\epsilon g)(x, y)$ denotes the erosion of the image f using the structuring element g , where the inverted union (\bigwedge) operation is applied over the (s, t) in set E_g defined by the structuring element. Both fits and hits operations contribute to the refinement of segmented regions by adjusting the boundaries and ensuring smoother transitions between adjacent regions. The choice of a 5×5 kernel size is influenced by the balance between preserving fine details and mitigating noise in the image. The morphological process results are given in fig 5 .

The morphologically processed images undergo a shuffling operation in the final stages of the preprocessing pipeline. By increasing the dataset's diversity and randomness, shuffling helps to strengthen the training process for the ensuing deep learning models. The dataset is carefully divided into training and testing sets in an 80:20 ratio after shuffling. This partitioning technique keeps a separate set of data for objective assessment and guarantees a sufficient amount for model training. Four different deep learning models are then fed the prepared datasets: DenseNet-201, EfficientNetB7, ResNet-50, and MobileNetV2. Fine-tuning is also applied to make the models configure to the dataset used. These models are used to examine and pick up patterns from the processed eye-tracking scan paths because they are well-known for their effectiveness in image classification tasks. The accuracy of each model is used to gauge its performance. The evaluation results of the models indicate that DenseNet-201 is the most accurate model out of the four, with an accuracy of 94.97%.

IV. RESULTS AND DISCUSSION

The networks' performance is evaluated using accuracy.

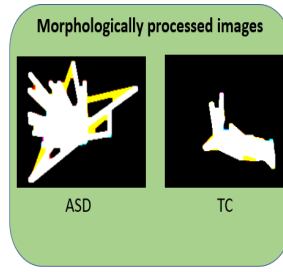


Fig. 5: Morphologically processed images

A. ACCURACY

A model's ability to predict an output given an input is known as its accuracy. Accuracy can be expressed as:

$$\text{Accuracy} = \frac{TP + TN}{TP + TN + FP + FN} \quad (9)$$

The superiority of k-means clustering in efficiently clustering pixels based on similarity makes it a viable option for segmentation. Resizing the images to fit the neural network requirements was carried out as the first step. This was followed by application of two prominent: Mean and Laplacian, to minimize noise and optimize data quality. Through image smoothing, the average filter, featuring a 5x5 filter size, lowers high-frequency noise and improves overall image clarity. The Laplacian filter is used alongside with other filters to accentuate edges, small details, and changes in intensity. Following that, the dataset is segmented using the k-means segmentation algorithm. Additionally, contrast stretching is used to increase the images' contrast. Morphological operations are carried out to further improve the processed images after image segmentation. In particular, the nearby intersection test (also known as hits) and adjacent union test (also known as fits) are applied in that order. The improved pictures are then shuffled around at random. The dataset is then meticulously divided into training and testing sets, maintaining an 80:20 ratio. Four deep learning models are then fed the preprocessed and partitioned datasets: DenseNet-201, EfficientNet B7, ResNet-50, and MobileNetV2. The accuracy of each model is used to assess its performance.

TABLE I: ACCURACY OF DIFFERENT MODELS

Model	Accuracy
DenseNet-201	94.97%
EfficientNet B7	94.74%
ResNet-50	92.45%
MobileNet V2	84.21%

The accuracy of the models is summarized in Table I. With accuracy of 94.97% and 94.74%, respectively, DenseNet-201 and EfficientNet B7 are the two models that perform the best. This shows that, based on the available eye tracking data, these models typically work well in identifying ASD. This result shows how successfully DenseNet-201 performs the specific task of identifying ASD by locating and logging pertinent elements inside the eye-tracking scan paths.

V. CONCLUSION

The study used deep learning models DenseNet-201, EfficientNet B7, ResNet-50, and MobileNetV2 to detect ASD using eye tracking technologies. This study significantly contributes to research community by highlighting the benefits of utilizing the pre-trained deep learning models in analyzing eye tracking scanpaths of autism affected individuals with accuracies of 94.97%, 94.74%, 84.21%, and 92.45%, respectively, the models showed encouraging results. Especially, the novel approach of usage of complex deep learning models DenseNet-201 and EfficientNet B7 which are the models with best performance among the models used. The model with the highest accuracy was DenseNet-201, which attained 94.97%. The important contribution of this research towards medical society and people is to improve our understanding of the detection of ASD along with other neurodevelopmental disorders paving way for early detection of autism as abnormal eye movement is a significant biomarker and visible symptom among children and benefitting medical and neuroimaging fields.

VI. FUTURE SCOPE

The work proposes the use of pre-trained models including DenseNet-201 and EfficientNet B7 and assess their performance. However, there is scope for improvement to fully understand and leverage their potential. Ensembling learning can be employed to improve the model's performance further. Also, the disturbances and other external factors might affect the capturing of eye tracking scanpaths and while applying the models to more large, diverse dataset. Therefore, more number of preprocessing steps and models fine-tuning techniques can be explored. Further, in the task of autism detection, the potential of these DenseNet-201 and Efficient B7 can be tested in brain scan images including MRI and CT scan images also.

REFERENCES

- [1] F. Ke, S. Choi, Y. H. Kang, K. Cheon, and S. W. Lee, "Exploring the structural and strategic bases of autism spectrum disorders with deep learning," *IEEE Access*, vol. 8, pp. 153341–153352, August 2020.
- [2] R. N. S. Husna, A. R. Syafeeza, N. A. Hamid, Y. C. Wong, and R. A. Raihan, "Functional magnetic resonance imaging for autism spectrum disorder detection using deep learning," *Jurnal Teknologi*, vol. 83, no. 3, pp. 45–52, April 2021.
- [3] T. Wadhera and D. Kakkar, "Eye Tracker," in *Advances in Medical Technologies and Clinical Practice Book Series*, pp. 125–152, 2019.

- [4] E. C. Bacon, A. Moore, Q. Lee, C. Barnes, E. Courchesne, and K. Pierce, "Identifying prognostic markers in autism spectrum disorder using eye tracking," *Autism*, vol. 24, no. 3, pp. 658–669, April 2020.
- [5] V. Yaneva, L. A. Ha, S. Eraslan, Y. Yesilada, and R. Mitkov, "Detecting high-functioning autism in adults using eye tracking and machine learning," *IEEE Trans. Neural Syst. Rehabil. Eng.*, vol. 28, no. 6, pp. 1254–1261, June 2020.
- [6] J. S. Oliveira, F. O. Franco, M. C. Revers, A. F. Silva, J. Portolese, H. Brentani, A. Machado-Lima, and F. L. S. Nunes, "Computer-aided autism diagnosis based on visual attention models using eye tracking," *Sci. Rep.*, vol. 11, no. 1, p. 10131, May 2021.
- [7] G. Wan, X. Kong, B. Sun, S. Yu, Y. Tu, J. Park, C. Lang, M. Koh, Z. Wei, Z. Feng, Y. Lin, and J. Kong, "Applying eye tracking to identify autism spectrum disorder in children," *J. Autism Dev. Disord.*, vol. 49, no. 1, pp. 209–215, January 2019.
- [8] I. A. Ahmed, E. M. Senan, T. H. Rassem, M. A. H. Ali, H. S. A. Shatnawi, S. M. Alwazer, and M. Alshahrani, "Eye tracking-based diagnosis and early detection of autism spectrum disorder using machine learning and deep learning techniques," *Electronics*, vol. 11, no. 4, p. 530, February 2022.
- [9] Z. Zhao, H. Tang, X. Zhang, X. Qu, X. Hu, and J. Lu, "Classification of children with autism and typical development using eye-tracking data from face-to-face conversations: Machine learning model development and performance evaluation," *J. Med. Internet Res.*, vol. 23, no. 8, p. e29328, August 2021.
- [10] M. R. Kanhirakadavath and M. S. M. Chandran, "Investigation of eye-tracking scan path as a biomarker for autism screening using machine learning algorithms," *Diagnostics*, vol. 12, no. 2, p. 518, February 2022.
- [11] J. Kang, X. Han, J. Song, Z. Niu, and X. Li, "The identification of children with autism spectrum disorder by SVM approach on EEG and eye-tracking data," *Comput. Biol. Med.*, vol. 120, p. 103722, May 2020.
- [12] M. Alcañiz, I. A. Chicchi-Giglioli, L. A. Carrasco-Ribelles, J. Marín-Morales, M. E. Minissi, G. Teruel-García, M. Sirera, and L. Abad, "Eye gaze as a biomarker in the recognition of autism spectrum disorder using virtual reality and machine learning: A proof of concept for diagnosis," *Autism Res.*, vol. 15, no. 1, pp. 131–145, January 2022.
- [13] S. Eraslan, Y. Yesilada, V. Yaneva, and S. Harper, "Autism detection based on eye movement sequences on the web: a scanpath trend analysis approach," in *Proceedings of the 17th International Web for All Conference (W4A '20)*, Article 11, pp. 1–10, April 2020.
- [14] M. A. R. Strobl, F. Lipsmeier, L. R. Demenescu, C. Gossens, M. Lindemann, and M. De Vos, "Look me in the eye: evaluating the accuracy of smartphone-based eye tracking for potential application in autism spectrum disorder research," *Biomed. Eng. Online*, vol. 18, no. 1, p. 51, May 2019.
- [15] R. Carette, M. Elbattah, F. Cilia, G. Dequen, J.-L. Guerin, and J. Bosche, "Learning to Predict Autism Spectrum Disorder based on the Visual Patterns of Eye-tracking Scanpaths," in *Proceedings of the 12th International Conference on Health Informatics*, pp. 103–112, February 2019.
- [16] M. E. Król and M. Król, "A novel machine learning analysis of eye-tracking data reveals suboptimal visual information extraction from facial stimuli in individuals with autism," *Neuropsychologia*, vol. 129, pp. 397–406, June 2019.
- [17] J. Kou, J. Le, M. Fu, C. Lan, Z. Chen, Q. Li, W. Zhao, L. Xu, B. Becker, and K. M. Kendrick, "Comparison of three different eye-tracking tasks for distinguishing autistic from typically developing children and autistic symptom severity," *Autism Res.*, vol. 12, no. 10, pp. 1529–1540, October 2019.
- [18] M. C. Pino, R. Vagnetti, M. Valenti, and M. Mazza, "Comparing virtual vs real faces expressing emotions in children with autism: An eye-tracking study," *Educational and Information Technologies*, vol. 26, no. 5, pp. 5717–5732, September 2021.
- [19] J. Vacas, A. Antolí, A. Sánchez-Raya, C. Pérez-Dueñas, and F. Cuadrado, "Visual preference for social vs. non-social images in young children with autism spectrum disorders: An eye tracking study," *PLoS One*, vol. 16, no. 6, p. e0252795, June 2021.
- [20] J. R. Yurkovic, G. Lisandrelli, R. C. Shaffer, K. C. Dominick, E. V. Pedapati, C. A. Erickson, D. P. Kennedy, and C. Yu, "Using head-mounted eye tracking to examine visual and manual exploration during naturalistic toy play in children with and without autism spectrum disorder," *Sci. Rep.*, vol. 11, no. 1, p. 3578, February 2021.